



RESEARCH PAPER

Arabidopsis ECHIDNA protein is involved in seed coloration, protein trafficking to vacuoles, and vacuolar biogenesis

Takuji Ichino^{1,2,3}, Kazuki Maeda¹, Ikuko Hara-Nishimura^{1,4}  and Tomoo Shimada^{1,*} 

¹ Department of Botany, Graduate School of Science, Kyoto University, Kyoto, 606–8502, Japan

² Department of Plant Developmental Biology, Centre for Organismal Studies, Heidelberg University, 69120 Heidelberg, Germany

³ Laboratory of Plant Gene Expression, Research Institute for Sustainable Humanosphere, Kyoto University, Uji, 611–0011, Japan

⁴ Department of Biology, Faculty of Science and Engineering, Konan University, Kobe, 658–8501, Japan

* Correspondence: tshimada@gr.bot.kyoto-u.ac.jp

Received 1 October 2019; Editorial decision 17 March 2020; Accepted 19 March 2020

Editor: Angus Murphy, University of Maryland, USA

Abstract

Flavonoids are a major group of plant-specific metabolites that determine flower and seed coloration. In plant cells, flavonoids are synthesized at the cytosolic surface of the endoplasmic reticulum and are sequestered in the vacuole. It is possible that membrane trafficking, including vesicle trafficking and organelle dynamics, contributes to flavonoid transport and accumulation. However, the underlying mechanism has yet to be fully elucidated. Here we show that the Arabidopsis ECHIDNA protein plays a role in flavonoid accumulation in the vacuole and protein trafficking to the vacuole. We found defective pigmentation patterns in *echidna* seed, possibly caused by reduced levels of proanthocyanidins, which determine seed coloration. The *echidna* mutant has defects in protein sorting to the protein storage vacuole as well as vacuole morphology. These findings indicate that ECHIDNA is involved in the vacuolar trafficking pathway as well as the previously described secretory pathway. In addition, we found a genetic interaction between *echidna* and *green fluorescent seed 9 (gfs9)*, a membrane trafficking factor involved in flavonoid accumulation. Our findings suggest that vacuolar trafficking and/or vacuolar development, both of which are collectively regulated by ECHIDNA and GFS9, are required for flavonoid accumulation, resulting in seed coat pigmentation.

Keywords: *Arabidopsis thaliana*, ECHIDNA, GREEN FLUORESCENT SEED 9, mucilage, protein sorting, seed coloration, *trans*-Golgi network, vacuolar morphology, vacuolar trafficking, vacuole

Introduction

A variety of metabolites unique to plants are produced as a plant strategy to adapt to the surrounding environment. Flavonoids are one group of secondary metabolites that are present in most land plants. Flavonoids act as pigments that determine flower and fruit coloration to attract pollinators and seed dispersers for plant reproduction and propagation (Kevan and Baker, 1983; Grotewold, 2006; Sheehan *et al.*, 2016). Plant seeds accumulate

flavonoids in their seed coats. Arabidopsis seed contains two types of flavonoids, flavonols and proanthocyanidins, also known as condensed tannins (Routaboul *et al.*, 2006). These seed flavonoids protect the embryo and endosperm inside the seed from pathogens and UV radiation. When flavonoid accumulation is blocked by the lack of associated molecular components, the seeds are pale tan in color, designated as *transparent*

Abbreviations: ER, endoplasmic reticulum; GFP, green fluorescent protein; GFS, GREEN FLUORESCENT SEED; PSV, protein storage vacuole; TGN, *trans*-Golgi network.

© The Author(s) 2020. Published by Oxford University Press on behalf of the Society for Experimental Biology. This is an Open Access article distributed under the terms of the Creative Commons Attribution License (<http://creativecommons.org/licenses/by/4.0/>), which permits unrestricted reuse, distribution, and reproduction in any medium, provided the original work is properly cited.

testa (*tt*) based on their mutant phenotype. Using genetic and molecular approaches, researchers have identified the detailed mechanism of flavonoid biosynthesis and its transcriptional regulation system (Lepiniec *et al.*, 2006).

Flavonoid biosynthesis starts in the phenylpropanoid pathway in plant cells. Most of the enzymes required for flavonoid biosynthesis form a protein complex referred to as the flavonoid metabolon and are located on the cytosolic surface of the endoplasmic reticulum (ER) membrane (Lepiniec *et al.*, 2006). Most flavonoids are amassed as pigments in the vacuole, where they are destined to be polymerized and chemically decorated by glycosylation, methylation, and acylation. The transport of flavonoids has been shown to involve membrane transporters located in endomembrane compartments. In *Arabidopsis thaliana*, the multidrug and toxic compound extrusion (MATE) family protein TT12 localizes on the vacuolar membrane of seed coat cells and functions in the uptake of flavonoid monomers into the vacuole (Debeaujon *et al.*, 2001; Marinova *et al.*, 2007). There are several orthologues of TT12 in *Vitis vinifera* and *Medicago truncatula* with flavonoid transport activity (Gomez *et al.*, 2009; Zhao and Dixon, 2009). The ATP-binding cassette proteins in *Zea mays*, *Glycine max*, and *V. vinifera* function in the transport of flavonoid derivatives across the membrane (Goodman *et al.*, 2004; Sugiyama *et al.*, 2007; Francisco *et al.*, 2013).

In addition to a transporter-mediated flavonoid transport system, vesicle-mediated trafficking is involved in flavonoid accumulation. In the tapetum cells of *Brassica* anthers, an ER-derived organelle, the tapetosome, contains flavonoids and lipids that are delivered to the pollen surface (Hsieh and Huang, 2007). The transport of anthocyanin, a pigmented flavonoid, to the vacuole in *Arabidopsis* leaf cells is affected by treatment with brefeldin A, an inhibitor of the vesicle trafficking machinery used for protein sorting (Poustka *et al.*, 2007). More recent observations have suggested that the machinery for autophagy, an intracellular recycling system, affects the vacuolar accumulation of anthocyanins (Kulich *et al.*, 2013). However, it remains controversial whether the autophagy-related components, which participate in the machinery for microautophagy, actually function in anthocyanin trafficking (Pourcel *et al.*, 2010; Chanoca *et al.*, 2015).

We have previously isolated the *Arabidopsis* mutant *green fluorescent seed 9* (*gfs9*) through forward genetic screening for protein trafficking to the vacuole (Fuji *et al.*, 2007). *gfs9* has a defect in seed coat pigmentation resulting from reduced accumulation of proanthocyanidins and flavonols in the seed (Ichino *et al.*, 2014). Identification of the gene responsible for *gfs9* revealed that *GFS9* is allelic to *TT9* (Shirley *et al.*, 1995; Ichino *et al.*, 2014). *GFS9* protein is distributed on the Golgi apparatus and functions in the trafficking of vacuolar proteins and in vacuolar development (Ichino *et al.*, 2014). Although analysis of *GFS9* has identified the role of the membrane trafficking machinery in flavonoid accumulation, the detailed mechanism linking membrane trafficking to flavonoid accumulation still is unknown. The question remains whether membrane trafficking factors other than *GFS9* are involved in flavonoid accumulation. It is also unclear whether any other

endomembrane compartments except for the Golgi apparatus affect flavonoid accumulation.

In this study, we identified another *Arabidopsis* trafficking mutant, *echidna*, which resulted in defective seed coloration, possibly as a result of reduced accumulation of proanthocyanidins. The *ECHIDNA* protein localizes to the *trans*-Golgi network (TGN) (Gendre *et al.*, 2011; Drakakaki *et al.*, 2012) and functions in secretory pathways, including the secretion of soluble apoplast proteins (Gendre *et al.*, 2011) and membrane proteins located on the plasma membrane, such as auxin carriers (e.g. *AUX1*, *PIN3*) (Boutte *et al.*, 2013). We found that a lack of *ECHIDNA* resulted in two kinds of membrane trafficking defects, in vacuolar protein sorting and vacuolar morphology. We also found an enhanced effect on plant growth with the combination of the *echidna* and *gfs9* mutations. These findings demonstrate that TGN-localized *ECHIDNA* and Golgi-localized *GFS9* orchestrate the intracellular trafficking of proteins and flavonoids, resulting in the regulation of plant development and seed coloration.

Materials and methods

Plant materials and growth conditions

We used *Arabidopsis thaliana* accessions Columbia-0 (CS60000) and Columbia-3 as the wild-type plants in this study. We used two lines of *Arabidopsis* T-DNA insertion mutants, *echidna* (SAIL_163_E09) and *gfs9-3* (SALK_057766, described as *gfs9* throughout this manuscript), which have been previously reported (Gendre *et al.*, 2011; Ichino *et al.*, 2014). The *Arabidopsis* seeds were surface-sterilized with 70% ethanol and then sown on to either 0.5% (w/v) gellan gum (Wako, Osaka, Japan) or 0.8% (w/v) agar containing 1% (w/v) sucrose and Murashige and Skoog medium (Wako). The seeds were incubated at 4 °C for 2 days to break seed dormancy. We grew the *Arabidopsis* plants side by side on plates at 22 °C for approximately 1 month under continuous light (100 μmol s⁻¹ m⁻²). Then, we transferred the plants on to vermiculite or peat moss (Sakata seed, Yokohama, Japan) for subsequent growth.

We crossed the *echidna* mutant with the *gfs9* mutant to generate the *echidna gfs9* double mutant. The F₂ plants were grown on a medium containing 10 mg l⁻¹ glufosinate ammonium (Sigma-Aldrich, St. Louis, USA) and 50 mg l⁻¹ kanamycin (Sigma-Aldrich) to select the plant lines bearing the T-DNA insertions in both the *ECHIDNA* and *GFS9* genes. After identifying the F₂ plants with the homozygous *gfs9* allele and the heterozygous *echidna* allele, we selected the *echidna gfs9* double mutant from the progeny of F₂ self-fertilization based on the *echidna* dwarf phenotype. The following *Arabidopsis* transgenic lines were also used: SP-GFP-CT24 (Fuji *et al.*, 2007), mCherry-VAMP711, and mCherry-ARA7 (Geldner *et al.*, 2009). We crossed the transgenic lines with the *echidna* mutant as described above to examine these proteins in the *echidna* mutant cell.

Genotyping

We identified T-DNA by PCR-based genotyping with genomic DNA extracted from the seedling leaves. We confirmed T-DNA insertion in the *ECHIDNA* gene (the *echidna* allele) by PCR using a combination of the primers LB1 (5'-AAA AATGAAGTTGTTTAAAGTAGGTA-3') and SAIL_163_E09-RP (5'-AGAGAAGAGTTATCGGGCTCG-3'). The wild-type allele in the *ECHIDNA* gene was confirmed by PCR using a combination of the primers SAIL_163_E09-LP (5'-AAACGGAAAGGGAAACACAAC-3') and SAIL_163_E09-RP. We confirmed the T-DNA insertion in the *GFS9* gene (the *gfs9* allele) by PCR using a combination of the primers LBa1 (5'-TGGTTCACGTAGTGGCCATCG-3') and At3g28430-4-R (5'-ATAGGCGGCTGCTCGGGTAA-3'). Finally, the wild-type

allele in *GFS9* was confirmed by PCR using a combination of the primers At3g28430-4-F (5'-GCCAGGGAAAGTCTCATCTGC-3') and At3g28430-4-R.

SDS-PAGE and immunoblot analysis

SDS-PAGE and immunoblot analysis were performed as described previously (Shimada *et al.*, 2003a, b). The dry seeds were homogenized with a pellet mixer (Treff, Degersheim, Switzerland) in 1× SDS sample buffer [50 mM Tris-HCl (pH 6.8), 1% (w/v) SDS, 5% 2-mercaptoethanol, 10% glycerol, 0.1% bromophenol blue]. The homogenates were heat-treated at 99 °C for 5 min. After centrifugation, the supernatant was analyzed using SDS-PAGE.

We used an anti-12S globulin antibody (diluted 10 000-fold) (Shimada *et al.*, 2003b) for immunoblotting. Signals were detected with an enhanced chemiluminescence detection system (GE Healthcare, Cambridge, UK) and LAS-3000 (Fujifilm, Tokyo, Japan).

Staining with *p*-dimethylaminocinnamaldehyde, propidium iodide, and india ink

To detect the accumulation of proanthocyanidin and its precursors, Arabidopsis seeds were stained with *p*-dimethylaminocinnamaldehyde as described in previous studies (Abrahams *et al.*, 2002; Baxter *et al.*, 2005). The dry seeds were stained with 2% (w/v) *p*-dimethylaminocinnamaldehyde (Tokyo Chemical Industry, Tokyo, Japan), 50% (w/v) methanol, and 3 M HCl for 1 week. Then, the stained seeds were washed four times in 70% (v/v) ethanol.

We used the fluorescent agent propidium iodide to detect root cap mucilage, as described previously (Rounds *et al.*, 2011; Maeda *et al.*, 2019). Seedlings 9 days after sowing were stained with 10 µg ml⁻¹ propidium iodide (Nacalai Tesque, Kyoto, Japan) for ~5 min and then mounted on a glass slide. The root caps were visualized under a confocal microscope.

The amount of root cap mucilage was quantified by staining with india ink, as described previously (Hawes *et al.*, 2000; Maeda *et al.*, 2019). We excised root tips (<1 cm) from vertically grown seedlings 9 days after sowing and placed them gently in 100 µl of 50% (v/v) india ink (Trusco Nakayama, Tokyo, Japan) on a glass slide using a toothpick. The unstained mucilage was observed using a light microscope (Axioskop 2 plus, Carl Zeiss, Jena, Germany) with a cover slip (24×60; Matsunami, Osaka, Japan) on the glass slide. We acquired images and segmented the images into regions representing mucilage or various tissues with ImageJ (<http://rsb.info.nih.gov/ij>) and its plugin, Trainable Weka Segmentation (Arganda-Carreras *et al.*, 2017).

Histological analysis

Root tips obtained from seedlings on day 9 after sowing were fixed with 4% (w/v) paraformaldehyde and 1% (v/v) glutaraldehyde in 50 mM cacodylate buffer (pH 7.4) for 2 hours. We followed the procedures described by Nishimura *et al.* (1993). The samples were dehydrated in a graded ethanol series at room temperature and embedded in LR White resin (London Resin, Basingstoke, UK). The blocks were polymerized under a UV lamp at -20 °C for 24 hours. We stained thin sections with toluidine blue and examined the sections with an Axioskop 2 plus light microscope.

Light microscopy

Arabidopsis seeds were observed by bright-field microscopy with a stereo microscope (SZX12; Olympus, Tokyo, Japan) equipped with a CCD camera (DP20; Olympus). To facilitate comparison of seed coloration, all images were acquired using the same parameters on the microscope and camera.

Fluorescent microscopy

We used a research Macro Zoom Fluorescence Microscope (MVX10; Olympus) equipped with a CCD camera (VB-7000; Keyence, Osaka,

Japan) to detect the green fluorescent protein (GFP) fluorescence in dry seeds expressing SP-GFP-CT24. We acquired all images using the same parameters on the microscope and camera to facilitate comparison of the intensity of fluorescence.

Confocal laser scanning microscopy

We removed the seed coat and endosperm from the seeds in glycerol to pick out the internal embryo in preparation to observe the GFP fluorescence of SP-GFP-CT24 and autofluorescence of protein storage vacuoles (PSVs). Seedlings were mounted in water on a microscope slide to prevent plasmolysis and examined using confocal laser scanning microscopy.

We used an LSM780 confocal laser scanning microscope (Carl Zeiss) to detect SP-GFP-CT24 fluorescence [excitation 488 nm (argon laser), emission 491–550 nm], mCherry-VAMP711 fluorescence, mCherry-ARA7 fluorescence, autofluorescence of PSVs [excitation 561 nm (diode-pumped solid-state laser), emission 560–656 nm], and the fluorescence of propidium iodide [excitation 561 nm (diode-pumped solid-state laser), emission 578–663 nm]. We captured images using a 63×1.20 numerical aperture water immersion objective (C-Apochromat, 441777-9970-000; Carl Zeiss).

We used another confocal laser scanning microscope (Leica TCS SP5 II, Leica Microsystems, Wetzlar, Germany) with a ×63.0 water immersion objective (HCX PL APO lambda blue 63.0×1.20 WATER UV; Leica) to visualize mCherry-ARA7 fluorescence [excitation 561 nm (DPSS laser), emission 615–676 nm] of the root cells. The acquired images were processed and analyzed using ZEN 2009 Light Edition, ZEN2011 Light Edition (Carl Zeiss), LAS AF Lite (Leica Microsystems), Adobe Photoshop Elements 9 (Adobe Systems, San Jose, USA), and ImageJ.

Statistical analysis

We analyzed multiple comparisons of seedling root length, plant height, and plant diameter using Tukey's honestly significant difference (HSD) test ($\alpha=0.01$) using the R 3.3.2 package (R Core Team, 2016). Multiple comparisons of PSV diameter and the signal intensity of mCherry-ARA7 were also analyzed by Tukey's HSD test ($\alpha=0.05$). Comparisons of the number and size of ARA7-positive endosomes, the ratio of signal intensity, deviation of PSV size, and area devoid of india ink were performed with Student's *t*-test.

Accession numbers

Arabidopsis Genome Initiative locus identifiers for the genes mentioned in this study are as follows: ECHIDNA, At1g09330; GFS9, At3g28430; VAMP711, At4g32150; ARA7, At4g19640.

Results

ECHIDNA is involved in seed coloration

Previously, we reported a molecular link between membrane trafficking and flavonoid accumulation in the vacuole (Ichino *et al.*, 2014). Further investigation revealed that the Arabidopsis trafficking mutant *echidna* produced grayish-tan seeds (Fig. 1A). Microscopic observation showed that *echidna* seeds exhibit a pale brown color with a partially whitish seed body (Fig. 1A). The wild-type seeds displayed a dark brown color throughout the whole seed body (Fig. 1A).

The coloration of plant seeds is determined by the quantity and quality of accumulated flavonoids. We stained the *echidna* seeds with *p*-dimethylaminocinnamaldehyde to detect the seed flavonoid proanthocyanidin. This reagent easily reacts with proanthocyanidins and its precursors to stain Arabidopsis seeds black (Abrahams *et al.*, 2002). After treatment with *p*-dimethy

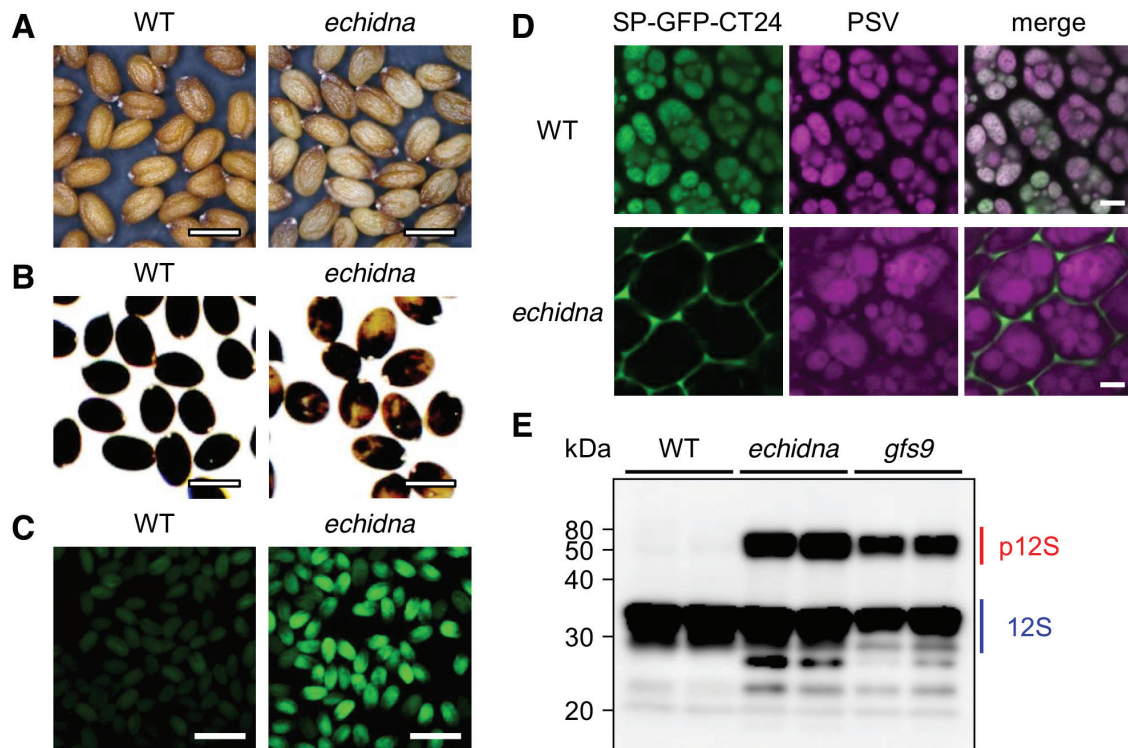


Fig. 1. Seed color phenotype and missorting of vacuolar proteins in *echidna* mutant seeds. (A) Seeds of wild-type (WT) and *echidna* mutant. (B) Seeds of WT and *echidna* mutant after staining with *p*-dimethylaminocinnamaldehyde. (C) GFP fluorescence images of WT and *echidna* dry seeds expressing vacuolar-targeted GFP, SP-GFP-CT24. (D) Confocal microscopic images of vacuolar-targeted GFP in embryonic cotyledon cells of WT and *echidna* dry seeds. Vacuolar-targeted GFP fluorescent signal and autofluorescence of the protein storage vacuole (PSV) are shown. (E) Immunoblot analysis of seed storage protein in WT, *echidna*, and *gfs9* seeds. Antibody to 12S globulin was used. The *gfs9* mutant is known to be defective in protein sorting to the vacuole. p12S, precursor forms of 12S globulin; 12S, mature form of 12S globulin. Bars=0.5 mm (A, B), 1 mm (C), and 5 μ m (D). (This figure is available in colour at *JXB* online.)

laminocinnamaldehyde, the wild-type seeds were completely stained black, whereas the *echidna* seeds were partially stained black (Fig. 1B). Some regions of *echidna* seed bodies were a tan color (Fig. 1B). These results suggest that ECHIDNA protein is required for seed coloration, possibly via a mechanism involving proanthocyanidin accumulation in the seeds.

ECHIDNA is involved in vacuolar protein sorting in seeds

ECHIDNA protein, which localizes to the TGN, has been shown to function in a secretory pathway to transport proteins and cell wall components, including polysaccharides, mucilage, and wax (Gendre *et al.*, 2011, 2013; McFarlane *et al.*, 2013, 2014). Currently, the involvement of ECHIDNA in vacuolar trafficking is unclear. Therefore, we investigated vacuolar protein sorting in *echidna* mutant seeds by introducing a vacuolar-targeted GFP, SP-GFP-CT24, which can trace the trafficking route to the PSV in seeds (Nishizawa *et al.*, 2003; Fuji *et al.*, 2007). *echidna* mutant seeds expressing SP-GFP-CT24 displayed strong GFP fluorescence, whereas wild-type seeds expressing SP-GFP-CT24 did not show any GFP fluorescence (Fig. 1C). This implies that SP-GFP-CT24 was missorted in the *echidna* mutant seeds because the missorting of SP-GFP-CT24 protein causes aberrant accumulation of this protein in the extracellular space and produces strong GFP fluorescence in seeds (Fuji *et al.*, 2007). In fact, SP-GFP-CT24 was abnormally secreted

to outside the cells in *echidna* seed cells (Fig. 1D). In contrast, SP-GFP-CT24 accumulated in PSVs in wild-type seed cells (Fig. 1D). These results suggest that vacuolar protein sorting to the PSV is compromised in the *echidna* mutant.

We performed an immunoblot analysis with anti-12S globulin antibody to identify defects of vacuolar sorting of endogenous proteins in *echidna* mutant seeds. 12S globulin is one of the major seed storage proteins; it is synthesized in the ER in its precursor form and then transported into the PSV, where it is converted into a mature form (Shimada *et al.*, 2003b). We predicted that defects in protein sorting in the vacuolar trafficking pathway would cause abnormal accumulation of the precursor form in dry seeds of *echidna* (Shimada *et al.*, 2003a). In wild-type seeds, 12S globulin appeared only in its mature form (Fig. 1E). In contrast, both the precursor form and the mature form of 12S globulin accumulated abnormally in the *echidna* mutant seeds; a similar pattern of accumulation was observed in *gfs9* mutant seeds (Fig. 1E). These findings confirm that ECHIDNA is involved in the vacuolar trafficking pathway in dry seeds.

We next examined the GFP fluorescence of SP-GFP-CT24 in *Arabidopsis* seedlings to determine whether ECHIDNA is involved in vacuolar protein transport in general or only in seeds. GFP fluorescence of SP-GFP-CT24 was rarely detected in the hypocotyl and root of both wild-type and *echidna* seedlings on the second day after germination (see Supplementary Fig. S1 at *JXB* online). This was probably due to the low

activity of the promoter of the α -subunit of β -conglycinin, a soybean seed storage protein, to express *SP-GFP-CT24* in these tissues of transgenic *Arabidopsis* (Nishizawa *et al.*, 2003). This promoter is known to express the *SP-GFP-CT24* gene in seeds but not in leaves of transgenic petunia plants (Beachy *et al.*, 1985). Therefore, we cannot conclude that ECHIDNA is involved in vacuolar protein transport in seedlings.

ECHIDNA is involved in the proper development of lytic vacuoles and protein storage vacuoles

We observed the vacuolar morphology in *echidna* mutant seedlings to investigate whether ECHIDNA protein has a role in vacuolar development. The fluorescent marker mCherry-fused VESICLE ASSOCIATED MEMBRANE PROTEIN 711 (VAMP711), which labels vacuolar membrane (Geldner *et al.*, 2009), was introduced into the *echidna* mutant. Using confocal microscopy, we found aberrant vacuolar morphology in *echidna* mutant cells (Fig. 2). mCherry-VAMP711 labeled the tonoplast of the central vacuole in root epidermal cells of wild-type seedlings (Fig. 2A, D). In contrast, mCherry-VAMP711 accumulated on aberrant structures in the immature epidermal

cells of *echidna* seedling roots, although VAMP711 also labeled central vacuolar membranes in the same cells (Fig. 2B). The aberrant structures present in immature cells of *echidna* roots had a much higher intensity of fluorescence than the central vacuolar membranes (Fig. 2B, C). The central vacuole of mature epidermal cells was expanded in both the wild-type and *echidna* mutant seedling roots (Fig. 2D, E). However, we found that the mature epidermal cells of *echidna* roots had abnormal membrane structures labeled by mCherry-VAMP711, which were not apparent in the wild-type cells (Fig. 2E, F).

The abnormal distribution of VAMP711 in the *echidna* mutant was apparent in both root cells and above-ground hypocotyl cells. mCherry-VAMP711 labeled the tonoplast in wild-type hypocotyl cells (Fig. 2G). In *echidna* hypocotyl cells, mCherry-VAMP711 labeled aberrant structures as well as the tonoplast (Fig. 2H). In the *echidna* hypocotyl, a variety of aberrant structures were labeled by mCherry-VAMP711: multi-layered or multi-membrane structures, aggregations of membrane compartments, and unidentified structures (Fig. 2H, I, and Supplementary Fig. S2). These aberrant structures were usually greater than 10 μm in size. These observations demonstrate that vacuolar membrane forms the aberrant

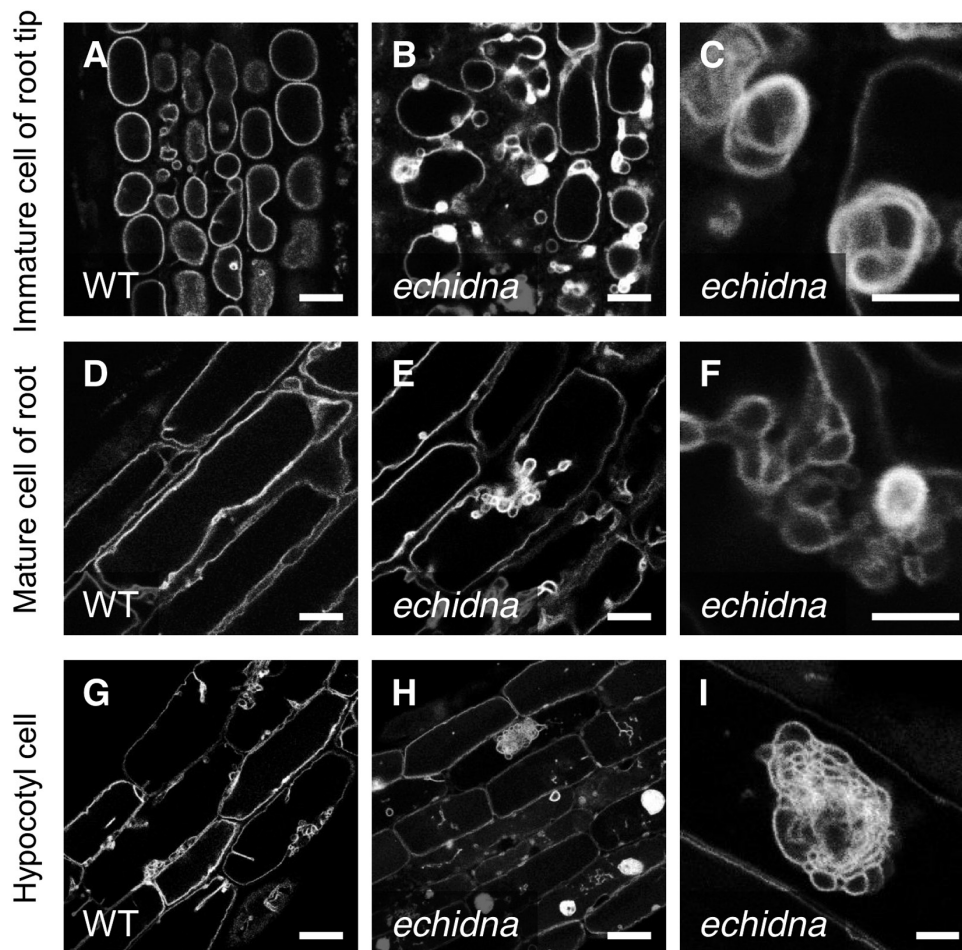


Fig. 2. Distribution of vacuolar membrane protein VAMP711 in the *echidna* mutant. Confocal microscopic images of the vacuolar membrane marker mCherry-VAMP711 in wild-type (WT) (A, D, G) and *echidna* mutant (B, C, E, F, H, I) cells. (A–C) Immature epidermal cells of root tip; (D–F) elongated (mature) epidermal cells of seedling root; (G–I) epidermal cells of hypocotyl. Images C, F, and I are magnified views of abnormal structures in the *echidna* mutant. The images in B and C were observed in different seedlings; images in E and F were observed in different fields of view from the same seedling; images in H and I were observed in different fields of view from the same seedling. Bars=10 μm (A, B, D, E), 5 μm (C, F, I), and 20 μm (G, H).

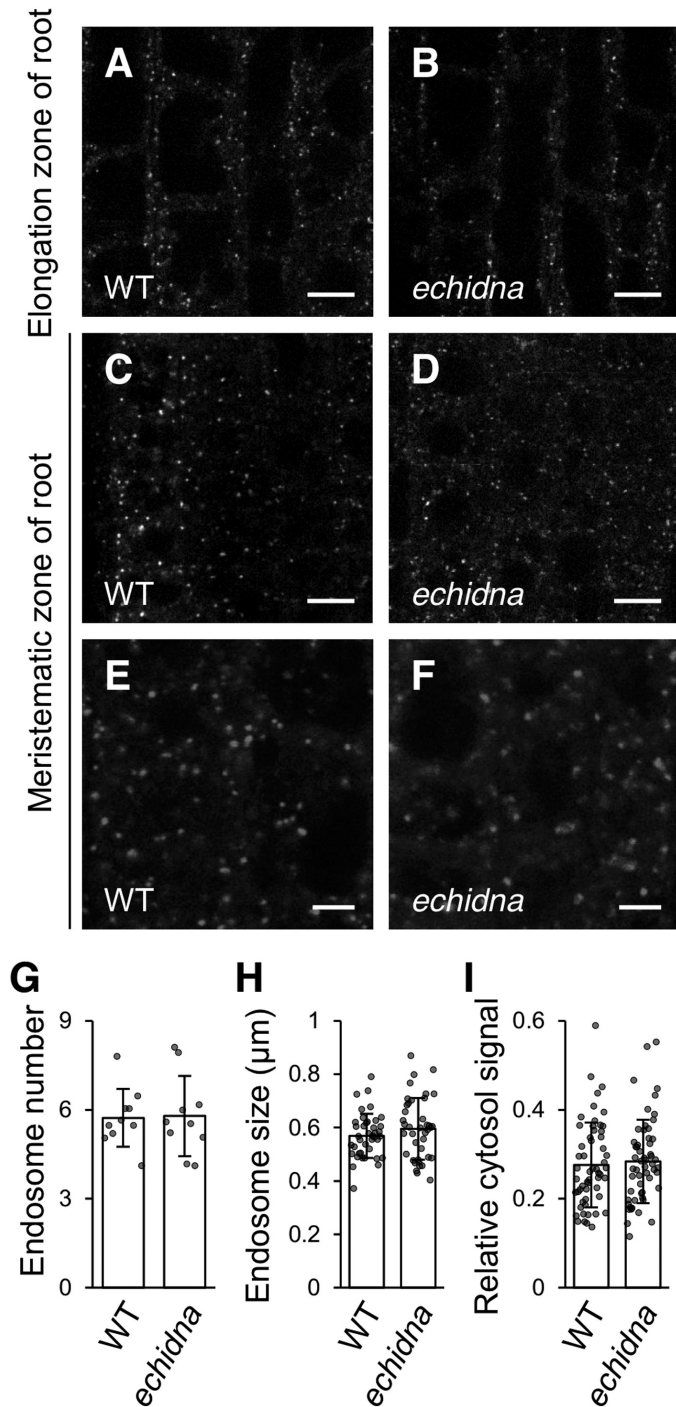


Fig. 3. ARA7-labeled late endosomes in the *echidna* mutant. (A–F) Confocal microscopic images of root cells from wild-type (WT) (A, C, E) and *echidna* mutant (B, D, F) seedlings. Late endosomes are labeled with mCherry-ARA7. (A, B) Root cells of the elongation zone; (C–F) root cells of the meristematic zone. Bars=10 μm (A–D) and 5 μm (E, F). (G) Number of ARA7-labeled late endosomes per 100 μm² area in root cells of the elongation zone. Ten plants of each genotype were measured. Each dot represents the mean of three to five regions of interest in a single plant. Each bar graph represents the mean of 10 means ±SD. (H) Size of ARA7-labeled late endosomes in the root cells of the elongation zone. Eight plants of each genotype were measured (five endosomes per plant). Each dot represents the size of a single endosome. Each bar graph represents the mean of 40 endosomes ±SD. (I) Relative signal intensity of cytosol fluorescence, calculated as the ratio of the intensity of cytosolic signal to the intensity of punctate structures within the same cell in the root

structures and aggregations in *echidna* mutant cells, which suggests that ECHIDNA is involved in the proper development of lytic vacuoles.

To examine the effect of ECHIDNA on the development of PSVs in seeds, we observed PSVs and quantitated their diameters (Supplementary Fig. S3). The largest PSV within *echidna* cells was significantly larger than that of wild-type cells, whereas the sizes of the other smaller PSVs within the same cell were comparable between *echidna* and wild-type cells (Supplementary Fig. S3B). The deviation in PSV size of the *echidna* seeds was larger than that of the wild-type seeds (Supplementary Fig. S3C), indicating that PSVs in *echidna* seed cells are more variable in size, whereas PSVs in wild-type seed cells are more uniformly sized. These results suggest that ECHIDNA is involved in regulating PSV morphology in seeds.

ECHIDNA does not affect late endosomal morphology

The *echidna* mutation causes morphological defects in several endomembrane compartments including the vacuole (Fig. 2), as well as ER and TGN (Gendre *et al.*, 2011; Boute *et al.*, 2013; McFarlane *et al.*, 2014; Ravikumar *et al.*, 2018). Therefore, we investigated whether ECHIDNA has an effect on the morphology of the late endosome. We introduced a fluorescent marker of the late endosome, mCherry-ARA7 (Geldner *et al.*, 2009), into the *echidna* mutant. Using confocal microscopy, we observed ARA7-labeled endosomes as punctate structures in elongated (Fig. 3A, B) and immature (Fig. 3C–F, and Supplementary Fig. S4A) root cells of *echidna* seedlings, similar to the wild-type seedlings. Quantitative analysis revealed no significant differences in the number and size of ARA7-labeled endosomes between wild-type and *echidna* mutant seedlings (Fig. 3G, H). The signal intensity of cytosolic fluorescence and relative intensities of cytosolic fluorescence compared with endosome fluorescence were similar between wild-type and *echidna* mutant seedlings (Fig. 3I and Supplementary Fig. S4B). These results suggest that ECHIDNA protein has little or no effect on late endosomal morphology.

ECHIDNA is involved in the local accumulation of root cap mucilage

Seed coat mucilage, a kind of polysaccharide that is secreted to the apoplast, has been shown to be inappropriately located in the vacuole in *echidna* seed coat cells (Gendre *et al.*, 2013; McFarlane *et al.*, 2013). We recently established efficient methods to detect root cap mucilage in Arabidopsis (Maeda *et al.*, 2019), and so we investigated the formation and secretion of root cap mucilage in *echidna* roots. First, we detected the periplasmic mucilage in wild-type and *echidna* seedling roots by staining with the fluorescent agent propidium iodide. Whereas periplasmic mucilage accumulated solely at

elongation zone. Fourteen plants of each genotype were measured (four cells per plant). Each dot represents the relative signal intensity of a single cell. Each bar graph represents the mean of 56 cells ±SD. *P* values were calculated using Student's *t*-test and were as follows: *P*=0.91 (G), *P*=0.24 (H), and *P*=0.66 (I).

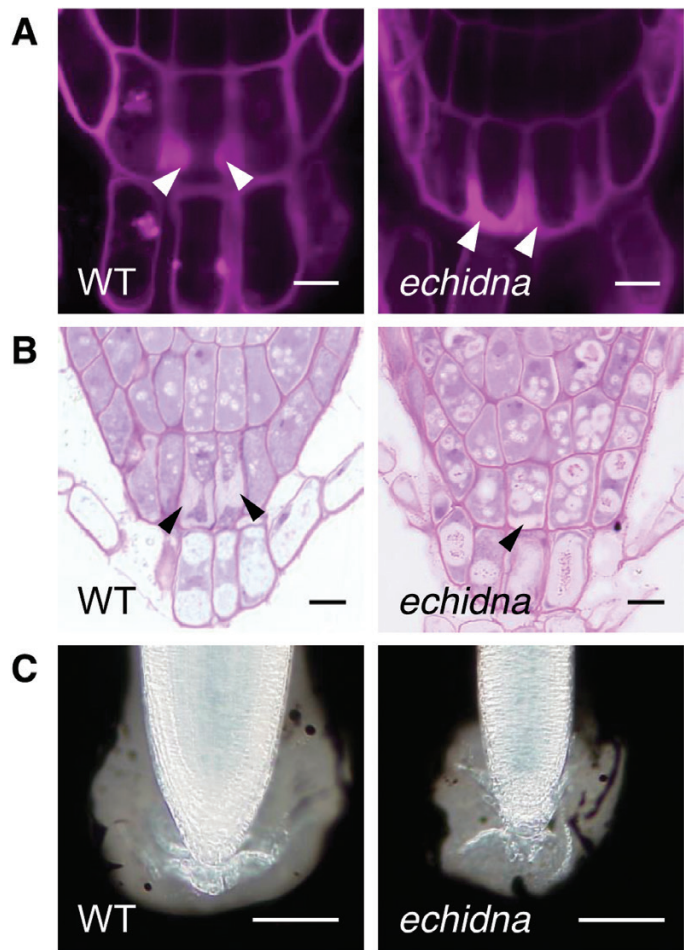


Fig. 4. Root cap mucilage in the *echidna* mutant. (A) Confocal microscopic images of the root tip of the wild-type (WT) and *echidna* mutant stained using propidium iodide. (B) Toluidine blue-stained sections of the root tip of the WT and *echidna* mutant. (C) Images of the root tip of the WT and *echidna* mutant stained using india ink. Arrowheads indicate periplasmic mucilage. Bars=10 μm (A, B) and 50 μm (C). (This figure is available in colour at JXB online.)

the lateral side of columella cells in wild-type roots, it accumulated on the lower side and lateral side of columella cells in *echidna* roots (Fig. 4A). This defect in the distribution of periplasmic mucilage in *echidna* columella cells was confirmed by staining cross sections of root tips with toluidine blue (Fig. 4B). Next, we quantified the amount of root cap mucilage by staining with india ink. The area devoid of india ink in *echidna* seedling roots was significantly smaller than that in wild type roots (Fig. 4C and Supplementary Fig. S5), suggesting that *echidna* roots secrete less mucilage than wild-type roots. This may be due to the smaller size of *echidna* roots rather than a secretion defect in *echidna* cells. Our results suggest that ECHIDNA is required for both the proper transport and local accumulation of root cap mucilage in the lateral side of columella cells.

ECHIDNA has a genetic interaction with GFS9

As described above, the *echidna* mutant has an effect on seed coloration, vacuolar trafficking (Fig. 1), and vacuolar morphology (Fig. 2). Similar phenotypes have been observed in

mutant cells lacking GFS9, which is a Golgi-localized protein responsible for several membrane trafficking events in the plant endomembrane system, such as protein trafficking to vacuoles, vacuolar development, and endosomal maturation (Ichino *et al.*, 2014). In *gfs9* seeds, the contents of proanthocyanidins and flavonols are reduced, resulting in tan-colored seeds (Ichino *et al.*, 2014). Vacuolar proteins are missorted to outside cells in *gfs9* seeds, similar to *echidna*: the vacuolar marker SP-GFP-CT24 and the endogenous vacuolar protein 12S globulin were secreted to the apoplast in dry seeds of the *gfs9* mutant (Ichino *et al.*, 2014). In addition, a number of smaller vacuoles are present in *gfs9* cells (Ichino *et al.*, 2014). These findings prompted us to investigate the relationship between ECHIDNA and GFS9.

We crossed *echidna* and *gfs9* to generate double mutant plants. The *echidna* mutant showed severe defects in plant growth, with a shorter seedling root, and a bushy and dwarf plant architecture (Fig. 5) (Gendre *et al.*, 2011; Fan *et al.*, 2014). The *gfs9* mutant also had a shorter seedling root, a slightly shorter plant height, and a smaller plant size than the wild type, but this phenotype was not as severe as that of the *echidna* mutant (Fig. 5 and Supplementary Fig. S6). The seedlings of the established *echidna gfs9* double mutant had a much shorter root length than that of either of the single mutants (Fig. 5A, B). At the mature adult stage, the *echidna gfs9* double mutant plant had severe growth defects and it did not produce fully expanded rosette leaves (Supplementary Fig. S6A, B). The plant height and size of the *echidna gfs9* double mutant were smaller than those of either of the single mutants (Fig. 5C, D and Supplementary Fig. S6A, B). Additionally, the double mutant was frequently unsuccessful in bolting inflorescence and flowering (Supplementary Fig. S6C, D), which resulted in defective seed production. These results demonstrated a synthetic genetic interaction between ECHIDNA and GFS9 in plant growth.

Discussion

In this study, we describe new roles of Arabidopsis ECHIDNA protein in seed coloration, protein trafficking to the vacuole (Fig. 1), and vacuolar development (Fig. 2). The absence of staining with *p*-dimethylaminocinnamaldehyde and tan color of *echidna* seeds suggest lower accumulation of proanthocyanidins, a type of flavonoid (Fig. 1A, B). In the flavonoid biosynthetic pathway, early biosynthetic steps are performed on the ER membrane, where multi-enzyme complexes for flavonoid biosynthesis, including chalcone synthase and chalcone isomerase, are located (Saslowky and Winkel-Shirley, 2001; Jørgensen *et al.*, 2005). Finally, most of the synthesized flavonoids accumulate in the vacuole. It is not yet known how the membrane trafficking component ECHIDNA affects the transport and accumulation of flavonoids. One possibility may be that vacuolar biogenesis, mediated by ECHIDNA, contributes to flavonoid accumulation in the vacuole. In the *echidna* mutant, invagination of mCherry-VAMP711-labels on the vacuolar membrane and aggregation with multiple membranes was evident in both hypocotyl and root cells (Fig. 2). A close connection

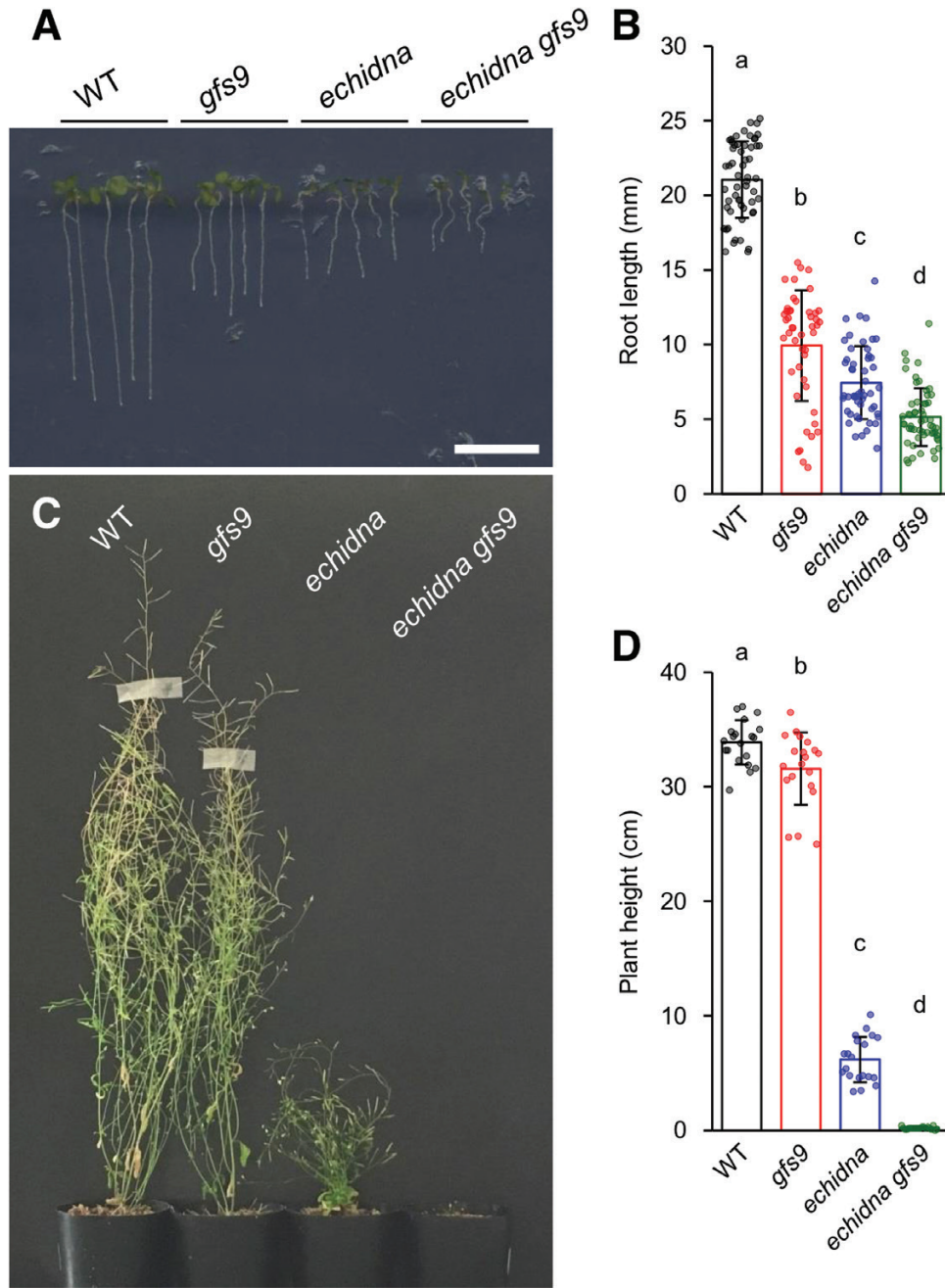


Fig. 5. Plant growth of *echidna*, *gfs9*, and the *echidna gfs9* double mutant. (A) Image of 5-day-old seedlings. Bar=1 cm. (B) Primary root length of 5-day-old seedlings. The numbers of measured seedlings of wild-type (WT), *gfs9*, *echidna*, and *echidna gfs9* were 56, 47, 51, and 56, respectively. (C) Image of 80-day-old fully mature adult plants. (D) Plant height of 51-day-old adult plants; 20 individuals of each genotype were measured. Data represent the mean \pm SD and raw data points. Different letters above the bars indicate statistically significant differences according to Tukey's HSD test for multiple comparisons ($\alpha=0.01$). (This figure is available in colour at JXB online.)

between vacuolar morphology and flavonoid accumulation has been reported in *Arabidopsis*. Multiple smaller vacuoles have been found in the seed coat cells, where proanthocyanidins are accumulated, of several flavonoid-deficient mutants, including a MATE-type transporter mutant *tt12* (Debeaujon *et al.*, 2001), P_{3A} -type H^+ -ATPase mutant *tt13/aha10* (Baxter *et al.*, 2005; Appelhagen *et al.*, 2015), leucoanthocyanidin dioxygenase mutant *tt18/tannin deficient seed 4* (Abrahams *et al.*, 2003), and glutathione-*S*-transferase mutant *tt19* (Kitamura *et al.*, 2004). In contrast, the chalcone synthase mutant *tt4* has a defect in vacuolar

biogenesis in hypocotyl cells (Rosado *et al.*, 2011), which implies that the flavonoid itself has effects on vacuolar development and integrity.

Another possibility is that ECHIDNA-mediated trafficking machinery is involved in flavonoid transport to the vacuole. The lack of ECHIDNA might cause missorting of flavonoids and, therefore, lead to reduced accumulation levels in the vacuole. It is possible that vacuolar proteins and flavonoids share the trafficking pathway from the ER to vacuole via the TGN, where the ECHIDNA protein is located. This idea is consistent with previous reports showing that the protein

trafficking route from ER to vacuole contributes to the vacuolar accumulation of anthocyanin (Poustka *et al.*, 2007; Rosado *et al.*, 2011). To date, two membrane trafficking components, GFS9 and SUPPRESSOR OF K⁺ TRANSPORT GROWTH DEFECT1 (SKD1), have been reported to affect seed coat pigmentation (Fig. 6). The Arabidopsis mutant lacking GFS9, which is associated with the Golgi apparatus, showed multiple phenotypes, including disrupted vacuolar protein sorting and the *transparent testa* phenotype (Ichino *et al.*, 2014). In addition, Arabidopsis plants expressing a dominant-negative version of SKD1, which is a subunit of the ESCRT machinery localized in the multivesicular body, showed defects in vacuolar protein sorting and seed coat pigmentation (Shahriari *et al.*, 2010a, b). These observations suggest that seed coat pigmentation might be dependent on membrane trafficking to the vacuole.

In addition to the above hypotheses, we cannot rule out the possibility that the seed color phenotype in the *echidna* mutant is caused by a defect in flavonoid biosynthesis on the ER. Previously, reduced wax biosynthesis has been reported in the defective mutant of ROOT HAIR DEFECTIVE3, which is responsible for ER organization (McFarlane *et al.*, 2014). Wax biosynthesis occurs in the ER, similar to flavonoid biosynthesis (Lee and Suh, 2013). ECHIDNA also affects ER morphology (McFarlane *et al.*, 2014). It is possible that the defective ER morphology in the *echidna* mutant disturbs flavonoid biosynthesis due to the disorganization of flavonoid metabolic enzymes on defective ER membranes.

In this study, we found a genetic interaction between *ECHIDNA* and *GFS9* (Fig. 5). The single mutants lacking either gene displayed multiple defects including plant growth, seed coloration, vacuolar trafficking, and vacuolar morphology. The *echidna gfs9* double mutant showed more severe defects in plant growth than either the *echidna* or the *gfs9* mutant alone (Fig. 5). This synthetic genetic interaction between *ECHIDNA* and *GFS9* in plant growth suggests two possibilities: either the two genes act in parallel pathways that converge at a node, or they act in successive steps of the same pathway (Pérez-Pérez *et al.*, 2009). *ECHIDNA* and *GFS9* might act in two different pathways for trafficking to the vacuole. Alternatively, *ECHIDNA* and *GFS9* might function in the same vacuolar trafficking pathway, residing at distinct compartments: *ECHIDNA* at the TGN and *GFS9* at the Golgi apparatus (Fig. 6). Probably due to their different locations, *ECHIDNA* and *GFS9* have different effects on vacuolar morphology. The *echidna* mutant has a single central vacuole with defective membrane dynamics (Fig. 2), while the *gfs9* mutant has multiple smaller vacuoles (Ichino *et al.*, 2014). Moreover, the aggregation in *echidna* showed vacuolar membrane identity (Fig. 2), while the aggregation in *gfs9* consists of enlarged late endosomes (Ichino *et al.*, 2014). The different effects of *ECHIDNA* and *GFS9* on vacuolar development could be explained by their distinct functions. *ECHIDNA* has been shown to maintain TGN integrity (Gendreau *et al.*, 2011; Boutte *et al.*, 2013). The lack of *ECHIDNA* caused the mislocalization of several TGN-localized proteins, including vacuolar H⁺-ATPase subunit a1 (Gendreau *et al.*, 2011). TGN integrity may underlie sequential vacuolar development, because plant endomembrane compartments originate and connect with each other. In plants, the TGN is derived from and

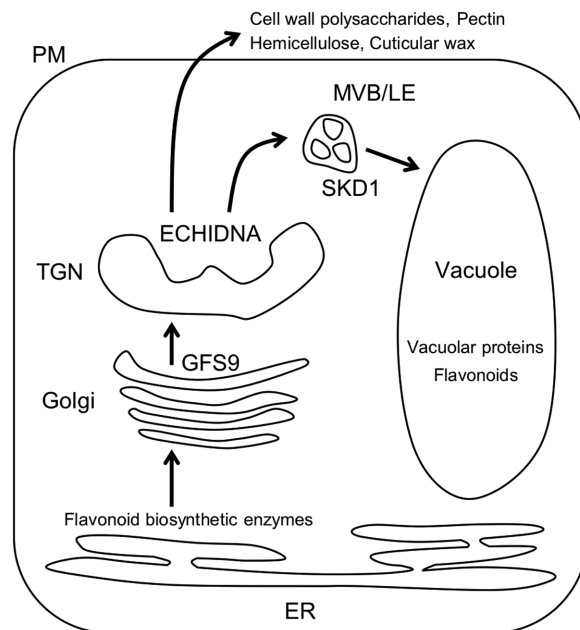


Fig. 6. Model of the intracellular trafficking pathway mediated by *ECHIDNA*. Early steps of flavonoid biosynthesis are performed on the endoplasmic reticulum (ER), and the final products (e.g. proanthocyanidins) accumulate in the vacuole. Vacuolar proteins (e.g. seed storage proteins) are also transported from the synthetic site on the ER to the final destination vacuole. GREEN FLUORESCENT SEED 9 (*GFS9*) on the Golgi apparatus and *ECHIDNA* on the *trans*-Golgi network (TGN) play roles in the trafficking of vacuolar proteins and flavonoids to the vacuole. *ECHIDNA* also mediates the secretion of cell wall components and cuticular wax. SUPPRESSOR OF K⁺ TRANSPORT GROWTH DEFECT1 (*SKD1*), a component of the ESCRT machinery on the multivesicular body (MVB)/late endosome (LE), has also been reported to be involved in the vacuolar trafficking of proteins and seed coat pigmentation. PM, plasma membrane.

associated with the Golgi apparatus (Stachelin and Kang, 2008; Uemura *et al.*, 2014), and a subdomain of the TGN matures to become a multivesicular body or late endosome (Scheuring *et al.*, 2011; Singh *et al.*, 2014). In contrast, the *gfs9* mutant may be defective in membrane fusion to the vacuole, because the *GFS9* orthologue of *Drosophila melanogaster* interacts with a subunit of the vacuolar tethering complex HOPS (Kim *et al.*, 2010). The HOPS complex is required for membrane fusion on the vacuole in Arabidopsis (Brillada *et al.*, 2018; Takemoto *et al.*, 2018).

We report a novel finding of the involvement of *ECHIDNA* in vacuolar trafficking of proteins (Fig. 1C–E). Together with the well-established function of *ECHIDNA* in protein secretion (Gendreau *et al.*, 2011; Boutte *et al.*, 2013), *ECHIDNA* has roles in distinct pathways—the vacuolar trafficking pathway and the secretory pathway—in the intracellular trafficking network of plant cells (Fig. 6). Misdistribution of SP-GFP-CT24 to the extracellular space was found in *echidna* seed cells (Fig. 1D), even though *ECHIDNA* is involved in secretion. This finding implies that the *echidna* mutant still has some activity in secretion. A previous report suggested that *ECHIDNA* is required for the route of secretory traffic defined by the secretion reporter *secGFP* but not for all secretory cargos (Gendreau *et al.*, 2011). Consistent with this notion, we found secretion of root cap mucilage from *echidna* mutant cells (Fig. 4). Moreover, the *echidna* mutant cell is able to form a cell wall, the construction of which is supported by the secretion of cell wall components.

The roles of ECHIDNA in the vacuolar and secretory trafficking pathways account for phytochemicals as well as proteins. Similar to its role in the vacuolar accumulation of flavonoids, ECHIDNA is involved in the secretion of cell wall polysaccharides (Fig. 4), pectin, hemicellulose (Gendre *et al.*, 2013; McFarlane *et al.*, 2013), and cuticular wax (McFarlane *et al.*, 2014). The molecular mechanism underlying the secretion of cell wall components has not been completely determined. Considering that ECHIDNA is required for multidirectional protein trafficking pathways, a similar mechanism may operate in ECHIDNA-mediated flavonoid accumulation in the vacuole and ECHIDNA-mediated secretion of cell wall components to the exterior of the cell. In fact, misdistribution of root cap mucilage (Fig. 4) and of pectin within the vacuole and ER (McFarlane *et al.*, 2013) has been observed in *echidna* seedling root and seed coat cells, respectively. This raises the possibility of misdistribution of flavonoids in *echidna* seed coat cells.

Our findings reveal that ECHIDNA has a role in multidirectional pathways of the intracellular trafficking network: the vacuolar trafficking pathway and the secretory pathway (Fig. 6). We report a new role of the plant TGN in vacuolar development and in the distribution of specialized metabolites of plants, including cell wall components and seed flavonoids. In addition, we show that ECHIDNA-mediated trafficking at the TGN and GFS9-mediated trafficking at the Golgi apparatus in tandem contribute to vacuolar trafficking and vacuolar development, which are required for flavonoid accumulation in plant seeds and for plant growth. Further research concerning the intracellular dynamics of plant specialized metabolites could result in the discovery of new roles of intracellular membrane compartments and networks.

Supplementary data

Supplementary data are available at *JXB* online.

Fig. S1. Confocal images of SP-GFP-CT24 in *echidna* seedlings.

Fig. S2. Confocal images of aberrant structures labeled with mCherry-VAMP711 in *echidna* hypocotyl cells.

Fig. S3. Quantitative analysis of protein storage vacuoles in *echidna* dry seeds.

Fig. S4. Confocal images and quantitative analysis of mCherry-ARA7-labeled late endosomes.

Fig. S5. Representative images converted by Trainable Weka segmentation and quantitative analysis of india ink staining.

Fig. S6. Plant size and reproductive growth of the *echidna gfs9* double mutant.

Acknowledgments

We are grateful to Dr Shigeru Utsumi and Dr Nobuyuki Maruyama (Kyoto University, Japan) for sharing *Arabidopsis* seeds of SP-GFP-CT24, and to the *Arabidopsis* Biological Resource Center (ABRC) at Ohio State University for providing *Arabidopsis* seeds of CS60000, Col-3, *echidna, gfs9-3*, mCherry-VAMP711, and mCherry-ARA7. We are also grateful to Dr Karin Schumacher and Dr Melanie Krebs (Heidelberg University, Germany) for their kind support to the confocal microscopic analysis, and to Dr Rishikesh P. Bhalerao (Swedish University of Agricultural Sciences, Sweden), Dr Makoto Shirakawa (Nara Institute

of Science and Technology, Japan), and Dr Kentaro Tamura (University of Shizuoka, Japan) for providing valuable advice about our research. This work was supported by Japan Society for the Promotion of Science grants to IH-N (no. JP22000014 and JP15H05776) and to TS (no. JP18K06284), and a JSPS fellowship to TI (no. JP11J01092). This work was also supported by Toyobo Biotechnology Foundation (Long-term Research Fellowship) to TI.

References

- Abrahams S, Lee E, Walker AR, Tanner GJ, Larkin PJ, Ashton AR. 2003. The *Arabidopsis* *TDS4* gene encodes leucoanthocyanidin dioxygenase (LDOX) and is essential for proanthocyanidin synthesis and vacuole development. *The Plant Journal* **35**, 624–636.
- Abrahams S, Tanner GJ, Larkin PJ, Ashton AR. 2002. Identification and biochemical characterization of mutants in the proanthocyanidin pathway in *Arabidopsis*. *Plant Physiology* **130**, 561–576.
- Appelhagen I, Nordholt N, Seidel T, Spelt K, Koes R, Quattrocchio F, Sagasser M, Weisshaar B. 2015. TRANSPARENT TESTA 13 is a tonoplast P_{3A}-ATPase required for vacuolar deposition of proanthocyanidins in *Arabidopsis thaliana* seeds. *The Plant Journal* **82**, 840–849.
- Arganda-Carreras I, Kaynig V, Rueden C, Eliceiri KW, Schindelin J, Cardona A, Sebastian Seung H. 2017. Trainable Weka Segmentation: a machine learning tool for microscopy pixel classification. *Bioinformatics* **33**, 2424–2426.
- Baxter IR, Young JC, Armstrong G, Foster N, Bogenschutz N, Cordova T, Peer WA, Hazen SP, Murphy AS, Harper JF. 2005. A plasma membrane H⁺-ATPase is required for the formation of proanthocyanidins in the seed coat endothelium of *Arabidopsis thaliana*. *Proceedings of the National Academy of Sciences, USA* **102**, 2649–2654.
- Beachy RN, Chen ZL, Horsch RB, Rogers SG, Hoffmann NJ, Fraley RT. 1985. Accumulation and assembly of soybean β -conglycinin in seeds of transformed petunia plants. *The EMBO Journal* **4**, 3047–3053.
- Boutté Y, Jonsson K, McFarlane HE, Johnson E, Gendre D, Swarup R, Friml J, Samuels L, Robert S, Bhalerao RP. 2013. ECHIDNA-mediated post-Golgi trafficking of auxin carriers for differential cell elongation. *Proceedings of the National Academy of Sciences, USA* **110**, 16259–16264.
- Brillada C, Zheng J, Krüger F, Rovira-Díaz E, Askani JC, Schumacher K, Rojas-Pierce M. 2018. Phosphoinositides control the localization of HOPS subunit VPS41, which together with VPS33 mediates vacuole fusion in plants. *Proceedings of the National Academy of Sciences, USA* **115**, E8305–E8314.
- Chanoca A, Kovinich N, Burkel B, Stecha S, Bohorquez-Restrepo A, Ueda T, Eliceiri KW, Grotewold E, Otegui MS. 2015. Anthocyanin vacuolar inclusions form by a microautophagy mechanism. *The Plant Cell* **27**, 2545–2559.
- Debeaujon I, Peeters AJ, Léon-Kloosterziel KM, Koornneef M. 2001. The *TRANSPARENT TESTA12* gene of *Arabidopsis* encodes a multidrug secondary transporter-like protein required for flavonoid sequestration in vacuoles of the seed coat endothelium. *The Plant Cell* **13**, 853–871.
- Drakakaki G, van de Ven W, Pan S, *et al.* 2012. Isolation and proteomic analysis of the SYP61 compartment reveal its role in exocytic trafficking in *Arabidopsis*. *Cell Research* **22**, 413–424.
- Fan X, Yang C, Klisch D, Ferguson A, Bhalerao RP, Niu X, Wilson ZA. 2014. ECHIDNA protein impacts on male fertility in *Arabidopsis* by mediating trans-Golgi network secretory trafficking during anther and pollen development. *Plant Physiology* **164**, 1338–1349.
- Francisco RM, Regalado A, Ageorges A, *et al.* 2013. ABCC1, an ATP binding cassette protein from grape berry, transports anthocyanidin 3-O-glucosides. *The Plant Cell* **25**, 1840–1854.
- Fuji K, Shimada T, Takahashi H, Tamura K, Koumoto Y, Utsumi S, Nishizawa K, Maruyama N, Hara-Nishimura I. 2007. *Arabidopsis* vacuolar sorting mutants (*green fluorescent seed*) can be identified efficiently by secretion of vacuole-targeted green fluorescent protein in their seeds. *The Plant Cell* **19**, 597–609.
- Geldner N, Dénervaud-Tendon V, Hyman DL, Mayer U, Stierhof YD, Chory J. 2009. Rapid, combinatorial analysis of membrane compartments in intact plants with a multicolor marker set. *The Plant Journal* **59**, 169–178.
- Gendre D, McFarlane HE, Johnson E, Mouille G, Sjödin A, Oh J, Levesque-Tremblay G, Watanabe Y, Samuels L, Bhalerao RP. 2013.

- Trans*-Golgi network localized ECHIDNA/Ypt interacting protein complex is required for the secretion of cell wall polysaccharides in *Arabidopsis*. *The Plant Cell* **25**, 2633–2646.
- Gendre D, Oh J, Boulté Y, et al.** 2011. Conserved *Arabidopsis* ECHIDNA protein mediates *trans*-Golgi-network trafficking and cell elongation. *Proceedings of the National Academy of Sciences, USA* **108**, 8048–8053.
- Gomez C, Terrier N, Torregrosa L, et al.** 2009. Grapevine MATE-type proteins act as vacuolar H⁺-dependent acylated anthocyanin transporters. *Plant Physiology* **150**, 402–415.
- Goodman CD, Casati P, Walbot V.** 2004. A multidrug resistance-associated protein involved in anthocyanin transport in *Zea mays*. *The Plant Cell* **16**, 1812–1826.
- Grotewold E.** 2006. The genetics and biochemistry of floral pigments. *Annual Review of Plant Biology* **57**, 761–780.
- Hawes MC, Gunawardena U, Miyasaka S, Zhao X.** 2000. The role of root border cells in plant defense. *Trends in Plant Science* **5**, 128–133.
- Hsieh K, Huang AH.** 2007. Tapetosomes in *Brassica* tapetum accumulate endoplasmic reticulum-derived flavonoids and alkanes for delivery to the pollen surface. *The Plant Cell* **19**, 582–596.
- Ichino T, Fuji K, Ueda H, et al.** 2014. GFS9/TT9 contributes to intracellular membrane trafficking and flavonoid accumulation in *Arabidopsis thaliana*. *The Plant Journal* **80**, 410–423.
- Jørgensen K, Rasmussen AV, Morant M, Nielsen AH, Bjarnholt N, Zagobelný M, Bak S, Møller BL.** 2005. Metabolon formation and metabolic channeling in the biosynthesis of plant natural products. *Current Opinion in Plant Biology* **8**, 280–291.
- Kevan PG, Baker HG.** 1983. Insects as flower visitors and pollinators. *Annual Review of Entomology* **28**, 407–453.
- Kim S, Wairkar YP, Daniels RW, DiAntonio A.** 2010. The novel endosomal membrane protein Ema interacts with the class C Vps–HOPS complex to promote endosomal maturation. *Journal of Cell Biology* **188**, 717–734.
- Kitamura S, Shikazono N, Tanaka A.** 2004. *TRANSPARENT TESTA 19* is involved in the accumulation of both anthocyanins and proanthocyanidins in *Arabidopsis*. *The Plant Journal* **37**, 104–114.
- Kulich I, Pečenková T, Sekereš J, Smetana O, Fendrych M, Foissner I, Höftberger M, Zárský V.** 2013. *Arabidopsis* exocyst subcomplex containing subunit EXO70B1 is involved in autophagy-related transport to the vacuole. *Traffic* **14**, 1155–1165.
- Lee SB, Suh MC.** 2013. Recent advances in cuticular wax biosynthesis and its regulation in *Arabidopsis*. *Molecular Plant* **6**, 246–249.
- Lepiniec L, Debeaujon I, Routaboul JM, Baudry A, Pourcel L, Nesi N, Caboche M.** 2006. Genetics and biochemistry of seed flavonoids. *Annual Review of Plant Biology* **57**, 405–430.
- Maeda K, Kunieda T, Tamura K, Hatano K, Hara-Nishimura I, Shimada T.** 2019. Identification of periplasmic root-cap mucilage in developing columella cells of *Arabidopsis thaliana*. *Plant & Cell Physiology* **60**, 1296–1303.
- Marinova K, Pourcel L, Weder B, Schwarz M, Barron D, Routaboul JM, Debeaujon I, Klein M.** 2007. The *Arabidopsis* MATE transporter TT12 acts as a vacuolar flavonoid/H⁺-antiporter active in proanthocyanidin-accumulating cells of the seed coat. *The Plant Cell* **19**, 2023–2038.
- McFarlane HE, Watanabe Y, Gendre D, Carruthers K, Levesque-Tremblay G, Haughn GW, Bhalerao RP, Samuels L.** 2013. Cell wall polysaccharides are mislocalized to the vacuole in *echidna* mutants. *Plant & Cell Physiology* **54**, 1867–1880.
- McFarlane HE, Watanabe Y, Yang W, Huang Y, Ohlrogge J, Samuels AL.** 2014. Golgi- and *trans*-Golgi network-mediated vesicle trafficking is required for wax secretion from epidermal cells. *Plant Physiology* **164**, 1250–1260.
- Nishimura M, Takeuchi Y, Debellis L, Hara-nishimura I.** 1993. Leaf peroxisomes are directly transformed to glyoxysomes during senescence of pumpkin cotyledons. *Protoplasma* **175**, 131–137.
- Nishizawa K, Maruyama N, Satoh R, Fuchikami Y, Higasa T, Utsumi S.** 2003. A C-terminal sequence of soybean β -conglycinin α' subunit acts as a vacuolar sorting determinant in seed cells. *The Plant Journal* **34**, 647–659.
- Pérez-Pérez JM, Candela H, Micó JL.** 2009. Understanding synergy in genetic interactions. *Trends in Genetics* **25**, 368–376.
- Pourcel L, Irani NG, Lu Y, Riedl K, Schwartz S, Grotewold E.** 2010. The formation of anthocyanic vacuolar inclusions in *Arabidopsis thaliana* and implications for the sequestration of anthocyanin pigments. *Molecular Plant* **3**, 78–90.
- Poustka F, Irani NG, Feller A, Lu Y, Pourcel L, Frame K, Grotewold E.** 2007. A trafficking pathway for anthocyanins overlaps with the endoplasmic reticulum-to-vacuole protein-sorting route in *Arabidopsis* and contributes to the formation of vacuolar inclusions. *Plant Physiology* **145**, 1323–1335.
- R Core Team.** 2016. R: A language and environment for statistical computing. Vienna: R Foundation for Statistical Computing. <https://www.R-project.org/>
- Ravikumar R, Kalbfuss N, Gendre D, et al.** 2018. Independent yet overlapping pathways ensure the robustness and responsiveness of *trans*-Golgi network functions in *Arabidopsis*. *Development* **145**, dev169201.
- Rosado A, Hicks GR, Norambuena L, et al.** 2011. Sortin1-hypersensitive mutants link vacuolar-trafficking defects and flavonoid metabolism in *Arabidopsis* vegetative tissues. *Chemistry & Biology* **18**, 187–197.
- Rounds CM, Lubeck E, Hepler PK, Winship LJ.** 2011. Propidium iodide competes with Ca²⁺ to label pectin in pollen tubes and *Arabidopsis* root hairs. *Plant Physiology* **157**, 175–187.
- Routaboul JM, Kerhoas L, Debeaujon I, Pourcel L, Caboche M, Einhorn J, Lepiniec L.** 2006. Flavonoid diversity and biosynthesis in seed of *Arabidopsis thaliana*. *Planta* **224**, 96–107.
- Saslowky D, Winkel-Shirley B.** 2001. Localization of flavonoid enzymes in *Arabidopsis* roots. *The Plant Journal* **27**, 37–48.
- Scheuring D, Viotti C, Krüger F, et al.** 2011. Multivesicular bodies mature from the *trans*-Golgi network/early endosome in *Arabidopsis*. *The Plant Cell* **23**, 3463–3481.
- Shahriari M, Hülskamp M, Schellmann S.** 2010. Seeds of *Arabidopsis* plants expressing dominant-negative AtSKD1 under control of the *GL2* promoter show a *transparent testa* phenotype and a mucilage defect. *Plant Signaling & Behavior* **5**, 1308–1310.
- Shahriari M, Keshavaiah C, Scheuring D, Sabovljevic A, Pimpl P, Häusler RE, Hülskamp M, Schellmann S.** 2010. The AAA-type ATPase AtSKD1 contributes to vacuolar maintenance of *Arabidopsis thaliana*. *The Plant Journal* **64**, 71–85.
- Sheehan H, Moser M, Klahre U, Esfeld K, Dell’Olive A, Mandel T, Metzger S, Vandenbussche M, Freitas L, Kuhlemeier C.** 2016. *MYB-FL* controls gain and loss of floral UV absorbance, a key trait affecting pollinator preference and reproductive isolation. *Nature Genetics* **48**, 159–166.
- Shimada T, Fuji K, Tamura K, Kondo M, Nishimura M, Hara-Nishimura I.** 2003. Vacuolar sorting receptor for seed storage proteins in *Arabidopsis thaliana*. *Proceedings of the National Academy of Sciences, USA* **100**, 16095–16100.
- Shimada T, Yamada K, Kataoka M, et al.** 2003. Vacuolar processing enzymes are essential for proper processing of seed storage proteins in *Arabidopsis thaliana*. *Journal of Biological Chemistry* **278**, 32292–32299.
- Shirley BW, Kubasek WL, Storz G, Bruggemann E, Koornneef M, Ausubel FM, Goodman HM.** 1995. Analysis of *Arabidopsis* mutants deficient in flavonoid biosynthesis. *The Plant Journal* **8**, 659–671.
- Singh MK, Krüger F, Beckmann H, et al.** 2014. Protein delivery to vacuole requires SAND protein-dependent Rab GTPase conversion for MVB-vacuole fusion. *Current Biology* **24**, 1383–1389.
- Staehelein LA, Kang BH.** 2008. Nanoscale architecture of endoplasmic reticulum export sites and of Golgi membranes as determined by electron tomography. *Plant Physiology* **147**, 1454–1468.
- Sugiyama A, Shitan N, Yazaki K.** 2007. Involvement of a soybean ATP-binding cassette-type transporter in the secretion of genistein, a signal flavonoid in legume-*Rhizobium* symbiosis. *Plant Physiology* **144**, 2000–2008.
- Takemoto K, Ebine K, Askani JC, Krüger F, Gonzalez ZA, Ito E, Goh T, Schumacher K, Nakano A, Ueda T.** 2018. Distinct sets of tethering complexes, SNARE complexes, and Rab GTPases mediate membrane fusion at the vacuole in *Arabidopsis*. *Proceedings of the National Academy of Sciences, USA* **115**, E2457–E2466.
- Uemura T, Suda Y, Ueda T, Nakano A.** 2014. Dynamic behavior of the *trans*-golgi network in root tissues of *Arabidopsis* revealed by super-resolution live imaging. *Plant & Cell Physiology* **55**, 694–703.
- Zhao J, Dixon RA.** 2009. MATE transporters facilitate vacuolar uptake of epicatechin 3'-O-glucoside for proanthocyanidin biosynthesis in *Medicago truncatula* and *Arabidopsis*. *The Plant Cell* **21**, 2323–2340.